




Effect of Addition of Previously-Synthesized Ce-TZP/Al₂O₃ Submicrometric Powder on the Properties of Al₂O₃-Based Ceramics

Anne Caroline de Paula Nascimento^a, Maycol Moreira Coutinho^a,
Manuel Felliipe Rodrigues Pais Alves^b , Claudinei dos Santos^{b*} ,
Jorge Luiz de Almeida Ferreira^a, Cosme Roberto M. Silva^a 

^aUniversidade de Brasília (UnB), Faculdade de Tecnologia, Asa Norte, 70.910-900, Brasília, DF, Brasil.

^bUniversidade do Estado do Rio de Janeiro (UERJ), Faculdade de Tecnologia (FAT), Rod. Presidente Dutra, km 298, 27.537-000, Resende, RJ, Brasil.

Received: October 02, 2021; Revised: December 08, 2021; Accepted: December 13, 2021

This work investigated the effect of a composite of tetragonal zirconia with alumina-reinforced Ceria (ATZ) previously synthesized, on the properties of alumina-based ceramics (Al₂O₃). Monolithic alumina powder and Al₂O₃ powder mixtures containing 5, 10, 15 and 20 wt.% of Ce-TZP/Al₂O₃ were processed by high energy milling, compacted and then sintered at 1600 °C - 2 h. Sintered pure alumina and composites were characterized by relative density, scanning electron microscopy, X-ray diffraction and surface roughness. Then, the elastic modulus, the Vickers hardness, the fracture toughness and the 4-point flexural strength were evaluated. The results indicated an increase in relative density as a function of the addition of ATZ, with values between 94.3 ± 0.8% and 98.9 ± 0.7%. The observed microstructure after sintering showed tetragonal ZrO₂ grains with average sizes of 0.6 μm well dispersed in the Al₂O₃ matrix, which presents average grain sizes of around 1.5 μm. The crystalline phases identified in the composites were ZrO₂-tetragonal and Al₂O₃ hexagonal. The addition of the composite (ATZ) in the alumina matrix generates a gradual reduction in the elastic modulus (398 ± 15 GPa ~366 ± 34 GPa) and in the hardness (20.5 ± 1 GPa ~17.3 ± 0.7 GPa) of the sintered ceramics. On the other hand, the addition of this same composite (ATZ) in the alumina matrix considerably increases the materials fracture toughness, reaching values of approximately 6.7 ± 0.9 MPa.m^{1/2}. The same trend was observed in the flexural strength results which ranged from 258 MPa (5wt.% Ce-TZP/Al₂O₃) to 316 MPa (20wt.% Ce,Y-TZP/Al₂O₃). The Ce-TZP reinforcement acts as a toughening agent of the Al₂O₃ matrix due to the coupled mechanisms of toughening by zirconia phase transformation, residual stresses due to the difference in thermal expansion of the crystalline phases and differences in microstructural morphologies.

Keywords: Zirconia-toughened alumina (ZTA), Ce-TZP reinforcement, Rietveld refinement, mechanical properties, coupled toughening mechanisms.

1. Introduction

Biomechanics is related to mechanical methods to investigate the function and movements of biological systems. It has been applied in orthopedic implant projects, being widely used in the evaluation of the function and performance of compatible biomaterials for use in the human body^{1,2}. Biomaterials have experienced considerable technological expansion, emerging as an innovation with the use of ceramic materials for this purpose, especially zirconia³⁻⁶. Ceramic materials that are used under severe loading and environmental conditions need to have their mechanical properties improved. The alumina, Al₂O₃, has been reinforced with yttria-stabilized zirconia (Y-TZP) because its mechanical strength is improved in an adequate way for the application. This type of material has been used in medical implants due to its biocompatibility,

high wear resistance and good toughness, in addition to its high hardness⁷⁻⁹.

Alumina-based ceramics have been widely used as a structural biomaterial, due to their high hardness, high elastic modulus, high wear resistance, and chemical stability at room temperature or at elevated temperatures. In counterpoint, alumina is known to be a brittle material, with low fracture toughness and flexural strength. Its low sinterability and microstructural characteristics discourage it from being used in more noble applications such as orthopedic prostheses, for example. Thus, a strategy adopted to improve its mechanical properties is the addition of a second phase that improves its strength and toughness. Among the potential candidates for mechanical reinforcement for alumina-matrix ceramics is tetragonal zirconia ceramic, *t*-ZrO₂^{10,11}. This ceramic is high strength and present high fracture toughness, because

*e-mail: claudineisvr@gmail.com

presents metastabilization of the tetragonal phase at room temperature. When the material is subjected to stress, the zirconia grains at the crack tip undergo a phase transformation, from tetragonal to monoclinic ($t \rightarrow m$). This transformation takes place with an increase in volume, creating compressive tensions in the regions near the end of the crack and behind it, which tends to close it, hindering its growth. Thus, the energy associated with crack propagation is dissipated by the $t \rightarrow m$ transformations¹²⁻¹⁶. However, if the zirconia is stabilized with yttria (Y-TZP) the meta-stabilization of the zirconia tetragonal phase can be impaired, both superficially and inside the specimen, due to the low temperature hydrothermal degradation (LTD) that occurs by changing the energy balance of the degraded grain. The $t \rightarrow m$ transformation may occur in this grain spontaneously or with small mechanical stimuli, giving rise to microcracks and loss of strength¹⁷⁻²⁰.

Although yttrium oxide (Y_2O_3) is the most used stabilizer, this stabilization of tetragonal-zirconia can also be obtained with other oxides, such as ceria oxide (CeO_2) which has already been reported as resistant to LTD¹³. Ceria-stabilized tetragonal polycrystalline zirconia (Ce-TZP) is a good alternative to Y-TZP ceramic, as it is resistant to hydrothermal degradation as it does not form hydrides in an aqueous medium and has much higher fracture toughness than Y-TZP ceramics. However, its flexural strength is considerably lower than that of Y-TZP, harming the material for structural applications^{15,16,21}.

In this context, several studies have been dedicated to investigate the addition of Al_2O_3 or hexaluminates to the Ce-TZP matrix, aiming to combine flexural strength and hardness in the same material. This behavior is obtained due to the high densification and the complex and refined microstructure present in these composites, which activates reinforcement mechanisms and allows the coupling of different toughening mechanisms, increasing the energy required for the crack propagation and, accordingly, increasing the material fracture resistance²²⁻²⁶.

The increased supply of ceramic raw materials with powders with regular morphological characteristics, with nanometric or submicrometric particle sizes, which present a high degree of homogeneity and dispersion, can be seen as a simple and viable alternative to improve the properties of brittle ceramics such as alumina, using relatively simple manufacturing routes, enabling more noble applications, where better mechanical properties are welcome. The objective of this work was to evaluate the influence of adding a commercial Ce-TZP/ Al_2O_3 powder to a ceramic matrix based on alumina (Al_2O_3) improving its densification and mechanical properties.

2. Experimental Procedure

2.1. Materials

In this study, alumina (Al_2O_3 CT3000LS) and the composite Ce-TZP/ Al_2O_3 were used, both commercial powders of high purity. The main characteristics of the raw materials are shown in Table 1.

2.2. Processing

Five distinct compositions of Alumina matrix ceramics were prepared, containing different amounts of

Table 1. Characteristics of the raw materials used in this work (Supplier data).

Material	Al_2O_3	Ce-TZP/ Al_2O_3
Designation/ Supplier	Alumina CT3000LS (Alcoa Group, USA)	ZirPro® Intense (Saint Gobain, France)
Al_2O_3 (wt.%)	99.88	25 ± 1
ZrO ₂ + HfO ₂ (wt.%)	-	64.5
CeO ₂ / Y ₂ O ₃ (90/10) (wt.%)	-	10.5 ± 0.5
SiO ₂ + Fe ₂ O ₃ + Na ₂ O (wt.%)	<0.05	<0.06
MgO (wt.%)	0.04	-
Density (g/cm ³)	3.95	5.56
Average Grain Size (μm) D50/D90	0.5 / 2.0	0.2 / 0.1

Ce-TZP/ Al_2O_3 powder (0, 5, 10, 15 and 20 wt.%). In order to homogenize the mixtures, the powders were added in a high energy attrition mill, for 1h at 250 rpm, using a 500 mL alumina jar and Ø10 mm spheres. In each mixture, 4wt.% of organic binder based on polyvinyl alcohol (0.04%) was added. Specimens (n = 10/group) with final dimensions of 5 mm x 5 mm x 50 mm were compacted by uniaxial pressing using a pressure of 100 MPa - 60 s.

The samples were sintered in a furnace with MoSi₂ resistors, model Naber-therm P310. In this step, a heating rate of 1 °C/min up to 300 °C with a 1h isotherm was used, followed by new heating with the same heating rate up to 750 °C and a 1h isotherm plateau. The final heating stage consisted of a heating rate of 5 °C/min to 1600 °C with a 2h isotherm. The adopted cooling rate was 5 °C/min to room temperature. The surfaces of the sintered specimens were standardized using traditional ceramographic preparation consisting of grinding followed by polishing using diamond paste from 15 to 3 μm.

2.3. Characterizations

The relative density was calculated by the relation between the apparent specific mass of the sintered samples, obtained by Archimedes' principle, and the theoretical specific mass of the compositions, calculated based on the rule of mixtures.

The crystalline phases present in the sintered samples were identified by X-ray diffraction, using the Panalytical diffractometer, model MRD PRO, with Co- α radiation, 40 KV power and 40 mA current. The diffraction data were collected at a 2-Theta range between 20° and 80°, with an angular step of 0,02° and an acquisition time of 100 seconds per step. The crystalline peaks were identified by comparison with standard crystallographic files, obtained from the database of inorganic crystallographic structures (ICSD - Institute FIZ Karlsruhe-Leibniz).

The microstructures of the composites were evaluated using scanning electron microscopy (JEOL JSM 7100 F microscope). The polished surfaces of the sintered samples were thermally etched at 1500 °C - 15 min to reveal the grain boundaries. Mean grain sizes were determined using the IMAGE J software, using Feret's diameter and sample space greater than 150 grains per composition.

The surface roughness analysis of the specimens was performed in a New View 7100 Profiler. The area of analysis was 0.470 μm × 0.350 μm. The roughness parameters used were:

- Ra - arithmetic average of the absolute values of the roughness points within the evaluation length
- Rz - average values of the five highest peaks and the five deepest valleys along the CP
- PV – Peak and Valley – average values of peaks and valleys in the analyzed space.

The methodology used to determine the Vickers hardness values followed ASTM C 1327 - 15²⁷. For statistical reasons, 21 Vickers impressions were made on the polished surfaces applying a load of 2000 gF (9.8N) for 10 s. Vickers microhardness tests were carried out using an Emco Test model DuraScan 20 microhardness tester, with a diamond indenter. The results were obtained using Equation 1:

$$H_V = 0.0018544 \cdot \frac{P}{l^2} \quad (1)$$

Where P is the applied load [N], l is the average value of the indentation diagonals (mm) and H_V is the microhardness (in GPa). The crack lengths measurements and the observation of their geometries were made just after the hardness test, seeking to avoid the slow growth of cracks, initiated by the stress field that acts after loading. To analyze the type of crack system acting during crack growth, the models proposed in Equations 2 and 3 were selected^{28,29}. The equation proposed by Casellas is indicated for the Palmqvist crack system and the equation proposed by Anstis should only be applied to systems that present half-penny cracks.

$$K_{IC} = 0,024 \cdot \left(\frac{E}{HV} \right)^{1/2} \cdot \frac{P}{c^{3/2}} \quad (2)$$

(System Palmqvist, $0,25 \leq c/a \leq 2,5$)

$$K_{IC} = 0,016 \cdot \left(\frac{E}{HV} \right)^{0,5} \cdot \frac{P}{c^{3/2}} \quad (3)$$

(System Half - penny, $c/a > 2,5$)

Where, K_{Ic} is the fracture toughness [MPa.m^{1/2}], E is the elastic modulus [GPa], H_V is the Vickers hardness [GPa], P is the indentation load [MPa], a is the semi diagonal of Vickers impression [m], l is the crack length [m]; “ c ” = “ $a + l$ ”.

The composites elastic modulus were determined by non-destructive acoustic testing using a Sonelastic IED model acoustic detection device (São Carlos, Brazil). This equipment is designed for flexural, torsional, longitudinal and planar vibration moduli, with frequencies between 20 and 96 kHz and for detectable elastic modulus up to 900 GPa.

The 4-point bending tests were carried out following the guidelines of ASTM C1161-13³⁰. Samples with dimensions of 5 mm x 5 mm x 45 mm were tested using roller spacing of 40 and 24 mm and loading rate of 0.5 mm/min in an

MTS Landmark with a 5 kN load cell. The flexural strength (modulus of rupture) values were calculated using Equation 4.

$$s = \frac{3PL}{4bd^2} \quad (4)$$

Where, P is the rupture load found in the test [N], L is the external extension of the support [mm], b is the width of the specimen [mm] and d is the specimen thickness [mm].

3. Results and Discussions

3.1. Physical and microstructural characterizations

The relative density values of the composite groups are shown in Figure 1. It is observed that the addition of the Ce-TZP/Al₂O₃ composite generates an evolution of densification, compared to the monolithic material, which presented an average relative density of 94.3 ± 0.7%. The addition of the ATZ mixture to the alumina matrix generates an improvement, with values in the range of 98 - 98.9% of the theoretical density. Among the groups of sintered composites, no considerable statistical differences were observed. However, the reduction in porosity improves the mechanical properties of ceramics, as will be seen later in this work.

Figure 2 shows the X-ray diffractograms of the different compositions. Figure 3 exhibits the respective results of the Rietveld Refinement. It is possible to observe, in all compositions, that the crystalline peaks of alumina (Al₂O₃) correspond to the Al₂O₃-hexagonal structure. Furthermore, the crystalline phase corresponding to zirconia detected in the composites has a tetragonal phase. Data provided by the manufacturer, as well as compiled in previous work⁷, indicate that the tetragonal zirconia matrix obtained after sintering comes from the stabilization caused by the CeO₂ present in the initial mixture of the material. The presence of ZrO₂-cubic as well as ZrO₂-monoclinic phase after sintering was not observed. Thus, it is considered that all ZrO₂ grains present

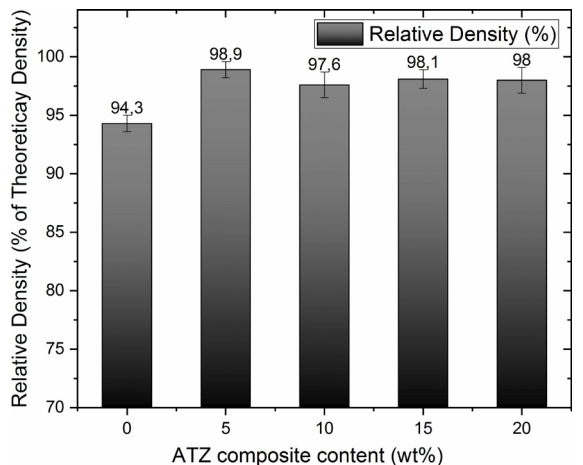


Figure 1. Relative density as a function against ATZ composite content in the Al₂O₃ matrix.

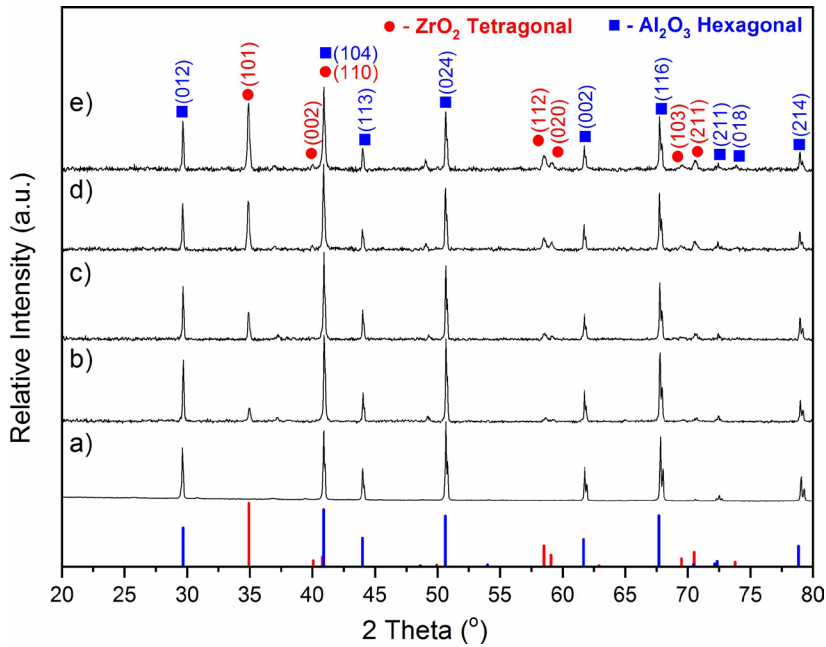


Figure 2. XRD patterns of the sintered samples : a) monolithic- Al_2O_3 -0%wt ATZ, b) Al_2O_3 -5wt.%ATZ, c) Al_2O_3 -10wt.%ATZ d) Al_2O_3 -15wt.%ATZ, e) Al_2O_3 -20wt.%ATZ. * Al_2O_3 (ICSD#9771); ZrO_2 Tetragonal (ICSD#66786).

in the composites have a tetragonal structure. The results shown in Figure 3 are indicative of the actual tetragonal zirconia content present in the composites. Note that the effective content of tetragonal zirconia in the alumina matrix ranges from 0 and 11.9% for proportions of up to 20 wt% of the ATZ powder (Ce-TZP/ Al_2O_3). Considering that this powder already contained 25% of Al_2O_3 , there is consistency between the final compositions of crystalline phases in the sintered composites. All properties evaluated in this manuscript will be studied as a function of the effective content of ZrO_2 -tetragonal stabilized with cerium (Ce-TZP).

Figure 4 shows representative micrographs of the sintered composites, with different ATZ contents, as well as the average grain size as a function of ATZ addition. It is possible to observe alumina grains with larger sizes, in the order of 1 to 2.5 μm , containing smaller tetragonal zirconia grains (close to 0.5 - 0.6 μm) dispersed homogeneously in the alumina matrix. The average size of zirconia grains observed in these composites is similar to those observed in previous works⁷ that used the same material and reinforcement, and, according to Basu¹³, this morphology presents an ideal sizes to optimize the shielding zone, responsible by toughening of tetragonal zirconia phase.

This homogeneity is an important factor in the context of guaranteeing the reliability of ceramic composites. The strategy adopted in this work was to use a previously synthesized commercial mixture that assures this good dispersion of Ce-TZP in the Al_2O_3 matrix. In conventional mixing/homogenization processes, typically long milling times (usually greater than 24 h) are required to achieve good homogeneity. Adopting the use of Ce-TZP/ Al_2O_3 mixtures used in this work, an efficient homogeneity was obtained with grinding for only 1 h in a planetary mill.

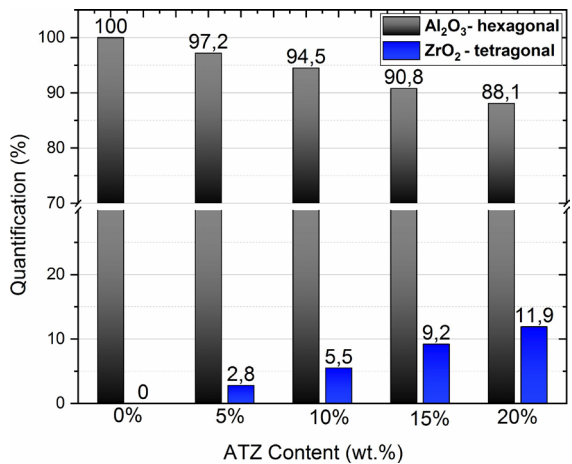


Figure 3. Rietveld refinement of the sintered samples for composites with different ATZ (Ce-TZP/ Al_2O_3) contents.

Figure 5 shows representative images of the 3D mapping of surface roughness for different materials submitted to bending tests. In addition, Figure 6 presents the results of the average roughness, Ra and Rz, and PV. The roughness parameters of Rz are clearly greater than Ra, Figure 6a. This difference was because Ra indicates the average roughness in the entire analyzed area, and larger peaks and valleys that appear on the surface will not significantly change Ra values. Conversely, Rz represents the average between the five highest peaks and deepest valleys in the analyzed area. As important as the Rz parameter is the surface PV parameter³¹, whose results are shown in Figure 6b. When

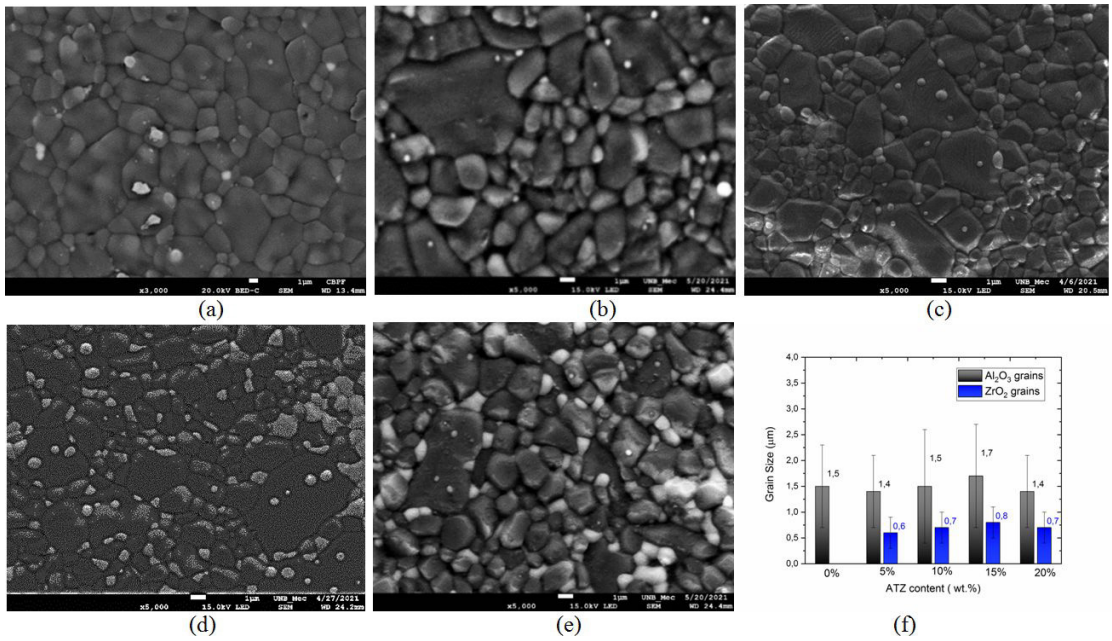


Figure 4. SEM micrographs of the composites a) monolithic Al_2O_3 -0% wt%ATZ, b) Al_2O_3 -5wt.%ATZ, c) Al_2O_3 -10wt.%ATZ d) Al_2O_3 -15wt.%ATZ, e) Al_2O_3 -20wt.%ATZ. (alumina as dark phase and zirconia as light phase).f) Average grain size of sintered composites as a function of ATZ addition.

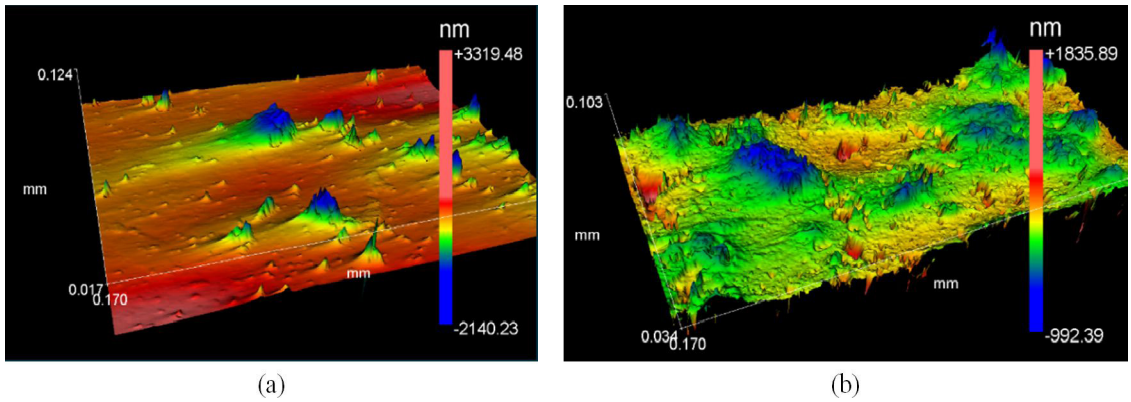


Figure 5. Example of 3D mapping of the roughness of ceramic composites: a) Al_2O_3 5wt.%ATZ, b) Al_2O_3 -20wt.%ATZ.

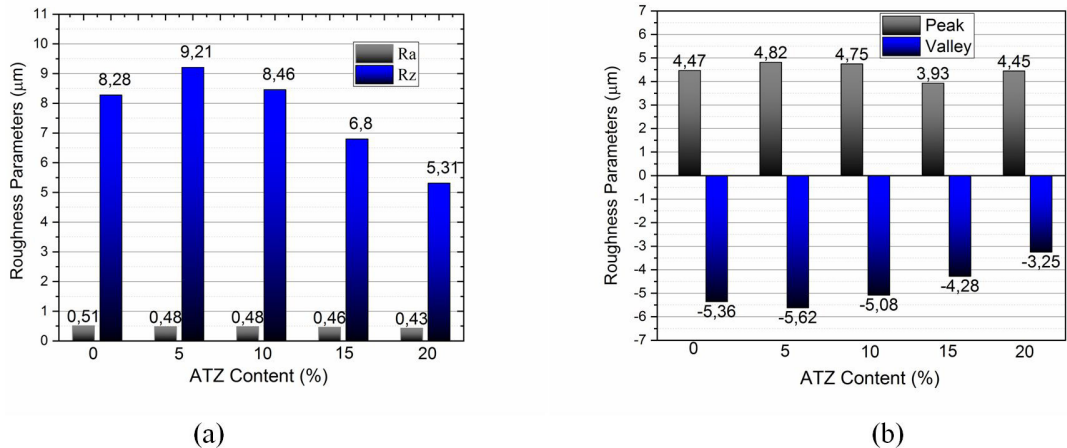


Figure 6. Roughness parameters of sintered ceramics: a) Ra and Rz; b) Peaks and valleys of Al_2O_3 samples sintered with different ATZ contents.

large peaks or valleys occur on the surface of the specimen, these changes can become significant stress concentrators, affecting flexural strength and fatigue values.

3.2. Mechanical properties

Figure 7 and Table 2 present the summary of the mechanical properties evaluated in this work.

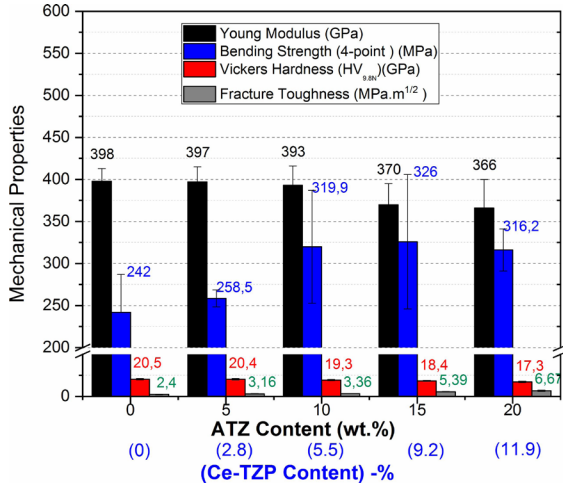


Figure 7. Hardness, fracture toughness, bending Strength and Young Modulus of the sintered zirconia toughened alumina (Ce-ATZ) ceramic composites.

It is possible to identify a decrease in the elastic modulus as a function of the Ce-TZP addition. Monolithic alumina has an elastic modulus close to 398 ± 15 GPa, while the addition of 11.9% Ce-TZP reduces this value to 366 ± 34 GPa. This result is consistent, since the modulus of elasticity of zirconia is approximately 190 - 200 GPa. Considering the theoretical hardness of the Al_2O_3 and ZrO_2 phases, around 21 GPa and 13 GPa, respectively, a reduction in the hardness of the composites as a function of the addition of Ce-TZP was observed in Figure 8. The values were in the range between 20.5 ± 1.0 and 17.3 ± 0.7 GPa.

The composites were characterized for hardness and fracture toughness by the Vickers indentation method, widely used due to its simplicity. The Vickers indenter produces cracks at the ends of the produced mark, as exemplified in Figure 8. The dimensions of these cracks can provide the fracture toughness of the material using specific formulas. Based on the experimental premises showed in Equations 2 and 3, the crack system was identified. In the materials studied, there is an alteration in the crack growth system due to the addition of tetragonal ZrO_2 stabilized with cerium (Ce-TZP) as reinforcement of the alumina matrix, see Table 2, column “c/a” ratio. At effective contents of up to 5.5% Ce-TZP, crack propagation in alumina ceramics is of the Half-penny type, characterized by a prevalence of brittle nature, with limited effect of toughening mechanisms.

In Table 2, the “c/a” ratio consistently decreases with the addition of Ce-TZP. At 9.2% or 11.9% Ce-TZP contents in the Al_2O_3 matrix, the “c/a” ratio suggests the growth of Palmqvist-

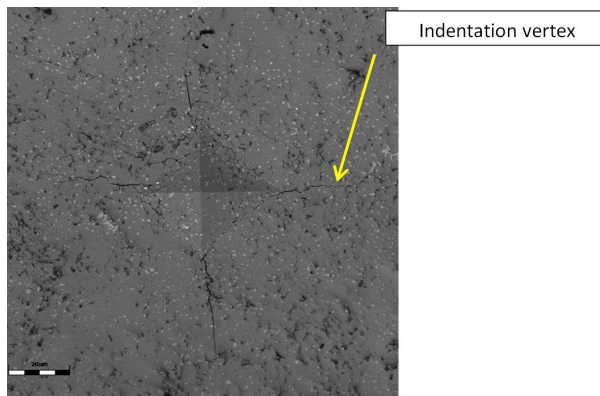


Figure 8. Vickers Indentation test result, showing microcracks in the indentation vertices.

Table 2. Summary of Mechanical Properties of the sintered zirconia-Toughened alumina (Ce-ZTA) ceramic composites as a function of Ce-TZP content.

Ce-TZP content (%)	Vickers Hardness (GPa) HV _{9.8N}	Crack ratio (c/a)	Fracture toughness (MPa.m ^{1/2})	Flexural strength (MPa)4-p	Elastic Modulus (GPa)
0%	20.5 ± 1.0	3.56 ± 0.27 (Half-penny)	2.40 ± 0.30	242 ± 45	398 ± 15
2.8%	20.4 ± 1.1	2.74 ± 0.15 (Half-penny)	3.16 ± 0.36	258.5 ± 10	397 ± 18
5.5%	19.3 ± 0.8	2.59 ± 0.11 (Half-penny)	3.36 ± 0.27	319.9 ± 67	393 ± 23
9.2%	18.4 ± 0.6	2.41 ± 0.13 (Palmqvist)	5.39 ± 0.38	326 ± 80	370 ± 25
11.9%	17.3 ± 0.7	2.09 ± 0.23 (Palmqvist)	6.67 ± 0.88	316.2 ± 25	366 ± 34

type cracks and, consequently, it is considered that crack propagation is more difficult. This behavior indicates increased fracture toughness of the material. In fact, observing Figure 8 and Table 2, it is noted that the fracture toughness values undergo a considerable increase, from $2.40 \pm 0.30 \text{ MPa}\cdot\text{m}^{1/2}$ (monolithic Al_2O_3) to $6.67 \pm 0.88 \text{ MPa}\cdot\text{m}^{1/2}$ (ZTA containing 11.9% Ce-TZP). The results indicate a 2.7-fold increase in the material toughness with Ce-TZP addition. In addition, the K_{IC} results presented in this study are consistent with ZTA composites, of the order of $5 \text{ MPa}\cdot\text{m}^{1/2}$, observed in the literature, highlighting that the composition with the highest amount of submicrometric Ce-TZP grains as reinforcement and the high densification, allowed values higher than those observed in the literature, but with flexural strength slightly lower³².

Zirconia-toughened alumina ceramics usually show similar behavior, with increase in fracture toughness due to the activation of the toughening mechanism by tetragonal to monoclinic ($t \rightarrow m$) phase transformation of the ZrO_2 grains dispersed in the alumina matrix. This behavior occurs because the tetragonal phase is metastable. When its grains are subjected to external stresses, as in the growth of a crack, it transforms into a monoclinic phase, which exhibits a volumetric expansion of about 3- 5%, with consequent compressive tension at the tip of the crack. At this moment, for the crack growth to continue, extra energy is required, which makes the material tougher than ceramics that do not present this behavior. In composites containing zirconia stabilized with 3mol % Y_2O_3 , 3Y-TZP, additions of up to 20%^{11,25} would be necessary to achieve similar results to those obtained in the present work.

The results presented in Table 2 and Figure 8 reveal the great toughening capacity of zirconia ceramics stabilized with

cerium, Ce-TZP. In this type of zirconia, cerium is the stabilizer, replacing the traditional Y_2O_3 . The chemical configuration of the tetragonal structure, and the consequent shielding zone at the crack tip of Ce-TZP systems, require higher energies than those needed for transformation into Y-TZP^{13,15,33}. This is because the shear stresses necessary for the destabilization of the structure are higher, contributing to the expansion of the shielding zone at the crack tip. Thus, considering that the grain size of both phases, Al_2O_3 and $t\text{-ZrO}_2$ does not change in the different sintered compositions, the increase in the population of Ce-TZP grains dispersed in the alumina matrix are responsible for the remarkable increase in the observed fracture toughness.

In addition to the retention of the tetragonal phase in the composite, this fracture toughness value can be attributed to the coupled toughening, that is, the association of different toughening mechanisms. Other mechanisms that can be attributed to this composite, in addition to the transformation that have already been mentioned, are the crack deflection, bridging and pull-out mechanism, due to the existence of a small concentration of cerium hexaluminate platelets present in the composite, and, as a result, hindering the crack growth^{13,21,34-36}.

It is also possible to verify the trend of an increase in the values of flexural strength as Ce-TZP is added to the compositions. According to Casellas et al.³⁷ increasing the zirconia content in the alumina matrix affects fracture strength. The addition of Ce-TZP in the alumina matrix changed the composite's behavior, probably due to phase transformation, with a strong influence on the mechanical properties of the alumina-zirconia composites.

Typical fracture surface profiles (4-point bending tests) are shown in Figure 9, for alumina-based ceramic samples with

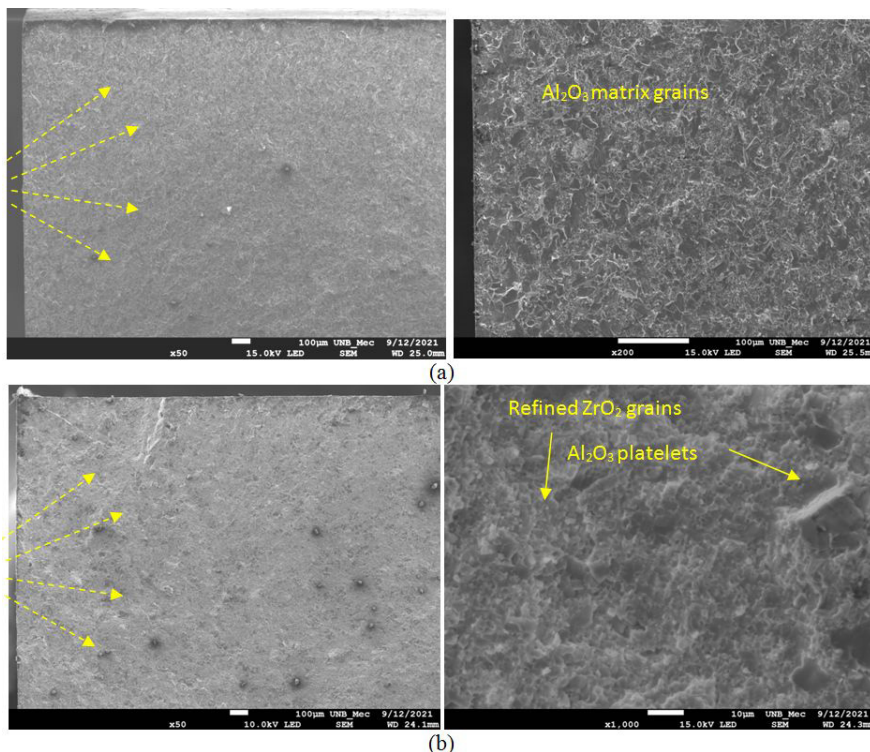


Figure 9. Fracture surface of ceramic composites containing: a) 5% ATZ (2.8% Ce-TZP); b) 20% ATZ (11.9% Ce-TZP).

small (5%) (Figure 9a) and considerable (20%) (Figure 9b) ATZ contents.

The fracture surface of the composite containing 5% ATZ has a more regular fracture profile, indicative of an intergranular fracture. Crack deflection from Al_2O_3 grains acts as the main toughening mechanism in this material. Actually, the population of Ce-TZP grains present in the overall material composition is reported to be 2.8%. Therefore, the transformation impacts of these grains on the microstructure is limited. On the other hand, the Al_2O_3 composite reinforced with 20% ATZ has a more irregular fracture profile, denoting the action of different mechanisms. It can be seen in Figure 9b that there are well-defined Al_2O_3 platelets whose crack growth requires extra energy for crack propagation. Additionally, the phase transformation on the fracture surface is an important mechanism to be considered, which allowed the increase of the material's toughness and flexural strength.

4. Conclusions

The addition of a previously synthesized submicrometric zirconia powder stabilized with ceria and reinforced with Al_2O_3 -Ce-TZP/ Al_2O_3 (up to 11.9wt. %) in the alumina matrix composite, ZTA, allowed to optimize the homogeneity of the mixture. Furthermore, it significantly improved the densification of Al_2O_3 -based ceramics. ZTA composites with a relative density of 99% were obtained after sintering at 1600 °C-2 h. The structural results indicated that hexagonal Al_2O_3 and tetragonal ZrO_2 had mean grain size of 1.5 μm and 0.6 μm , respectively. Composites containing 9.2wt.% Ce-TZP showed better flexural strength results (326 ± 80 MPa), while composites containing 11.9 wt.% Ce-TZP showed fracture toughness (K_{IC}) of 6.67 ± 0.9 MPa.m^{1/2}. These mechanical properties are significantly superior to those presented by monolithic- Al_2O_3 and the results are attributed to the presence of tetragonal submicrometric Ce-TZP grains which have toughening mechanisms by phase transformation, which allied to conventional crack-deflection mechanism and to the residual thermal stresses (resulting from the interaction between the Al_2O_3 and ZrO_2 phases), act to increase the strength and toughness of these ceramic composites.

5. Acknowledgments

The authors acknowledge Prof. Dr. Carlos Nelson Elias (Instituto Militar de Engenharia) for 3D-roughness measurements. Dr. Claudinei dos Santos thanks CNPq for the financial support (project 311119/2017-4) FAPERJ (grant E-26/202.997/2017).

6. References

- Hatze H. The meaning of the term biomechanics. *J Biomech.* 1974;7(2):189-90. [http://dx.doi.org/10.1016/0021-9290\(74\)90060-8](http://dx.doi.org/10.1016/0021-9290(74)90060-8). PMID:4837555.
- Zdero R, editor. *Experimental methods in orthopaedic biomechanics*. London: Academic Press; 2017. 401 p. <http://doi.org/10.1016/C2015-0-00572-X>.
- Sivaraman K, Chopra A, Narayan AI, Balakrishnan D. Is zirconia a viable alternative to titanium for oral implant? A critical review. *J Prosthodont Res.* 2018;62(2):121-33. <http://dx.doi.org/10.1016/j.jpor.2017.07.003>. PMID:28827030.
- Sanon C, Chevalier J, Douillard T, Cattani-Lorente M, Scherrer SS, Gremillard L. A new testing protocol for zirconia dental implants. *Dent Mater.* 2015;31(1):15-25. <http://dx.doi.org/10.1016/j.dental.2014.09.002>. PMID:25262212.
- Rahmati M, Mozafari M. A critical review on the cellular and molecular interactions at the interface of zirconia-based biomaterials. *Ceram Int.* 2018;44(14):16137-49. <http://dx.doi.org/10.1016/j.ceramint.2018.06.196>.
- Reveron H, Chevalier J. Yttria-stabilized zirconia as a biomaterial: from orthopedic towards dental applications. In: Pomeroy M, editor. *Encyclopedia of materials: technical ceramics and glasses*. Amsterdam: Elsevier; 2021. p. 540-52. (vol. 3).
- Santos C, Coutinho IF, Amarante JEV, Alves MFRP, Coutinho MM, Silva CRM. Mechanical properties of ceramic composites based on ZrO_2 co-stabilized by Y_2O_3 - CeO_2 reinforced with Al_2O_3 platelets for dental implants. *J Mech Behav Biomed Mater.* 2021;116(4):104372. <http://dx.doi.org/10.1016/j.jmbbm.2021.104372>. PMID:33540326.
- Moradkhani A, Baharvandi H. Effects of additive amount, testing method, fabrication process and sintering temperature on the mechanical properties of $\text{Al}_2\text{O}_3/3\text{Y-TZP}$ composites. *Eng Fract Mech.* 2018;191:446-60. <http://dx.doi.org/10.1016/j.engfracmech.2017.12.033>.
- Kurtz SM, Kocagöz S, Arnholt C, Huet R, Ueno M, Walter WL. Advances in zirconia toughened alumina biomaterials for total joint replacement. *J Mech Behav Biomed Mater.* 2014;31:107-16. <http://dx.doi.org/10.1016/j.jmbbm.2013.03.022>. PMID:23746930.
- Jalkh EBB, Coelho PG, Witek L, Bergamo ETP, Lopes ACO, Monteiro KN, al. Nanoscale physico-mechanical properties of an aging resistant ZTA composite. *J Mech Behav Biomed Mater.* 2021;123:104690. <http://dx.doi.org/10.1016/j.jmbbm.2021.104690>. PMID:34385065.
- Moraes MCCSB, Elias CN, Duailibi J Fo, Oliveira LG. Mechanical properties of alumina-zirconia composites for ceramic abutments. *Mater Res.* 2004;7(4):643-9. <http://dx.doi.org/10.1590/S1516-14392004000400021>.
- Chevalier J, Gremillard L, Virkar AV, Clarke DR. The tetragonal-monoclinic transformation in zirconia: lessons learned and future trends. *J Am Ceram Soc.* 2009;92(9):1901-20. <http://dx.doi.org/10.1111/j.1551-2916.2009.03278.x>.
- Basu B. Toughening of yttria-stabilised tetragonal zirconia ceramics. *Int Mater Rev.* 2005;50(4):239-56. <http://dx.doi.org/10.1179/174328005X41113>.
- Rejab NA, Azhar AZA, Ratnam MM, Ahmad ZA. The relation ship between microstructure and fracture toughness of zirconia toughened alumina (ZTA) added with MgO and CeO_2 . *Int J Refract Met Hard Mater.* 2013;41:522-30. <http://dx.doi.org/10.1016/j.ijrmhm.2013.07.002>.
- Rose LRF, Swain MV. Transformation zone shape in ceria partially-stabilized zirconia. *Acta Metall.* 1988;36(4):955-62. [http://dx.doi.org/10.1016/0001-6160\(88\)90150-2](http://dx.doi.org/10.1016/0001-6160(88)90150-2).
- Rauchs G, Fett T, Munz D, Oberacker R. Tetragonal-to-monoclinic phase transformation in CeO_2 -stabilised zirconia under uniaxial loading. *J Eur Ceram Soc.* 2001;21(12):2229-41. [http://dx.doi.org/10.1016/S0955-2219\(00\)00258-2](http://dx.doi.org/10.1016/S0955-2219(00)00258-2).
- Yoshimura M, Noma T, Kawabata K, Somiya S. Role of H_2O on the degradation process of Y-TZP. *J Mater Sci Lett.* 1987;6(4):465-7. <http://dx.doi.org/10.1007/BF01756800>.
- Ramesh S, Lee KYS, Tan CY. A review on the hydrothermal ageing behaviour of Y-TZP ceramics. *Ceram Int.* 2018;44(17):20620-34. <http://dx.doi.org/10.1016/j.ceramint.2018.08.216>.
- Abreu LG, Quintino MN, Alves MFRP, Habibe CH, Ramos AS, Santos C. Influence of the microstructure on the life prediction of hydrothermal degraded 3Y-TZP bioceramics. *J Mater Res Technol.* 2020;9(5):10830-40. <http://dx.doi.org/10.1016/j.jmrt.2020.07.059>.

20. Swab J. Low temperature degradation of Y-TZP materials. *J Mater Sci.* 1991;26(24):6706-14. <http://dx.doi.org/10.1007/BF02402664>.
21. Yu C-S, Shetty DK. Transformation zone shape, size, and crack-growth-resistance [r-curve] behavior of ceria-partially-stabilized zirconia polycrystals. *J Am Ceram Soc.* 1989;72(6):921-8. <http://dx.doi.org/10.1111/j.1151-2916.1989.tb06245.x>.
22. Fan K, Pastor JY, Ruiz-Hervias J, Gurauskis J, Baudin C. Determination of mechanical properties of Al₂O₃/Y-TZP ceramic composites: influence of testing method and residual stresses. *Ceram Int.* 2016;42(16):18700-10. <http://dx.doi.org/10.1016/j.ceramint.2016.09.008>.
23. Takano T, Tasaka A, Yoshinari M, Sakurai K. Fatigue strength of Ce-TZP/Al₂O₃ nanocomposite with different surfaces. *J Dent Res.* 2012;91(8):800-4. <http://dx.doi.org/10.1177/0022034512452277>. PMID:22736446.
24. Yang G, Li J-C, Wang G-C, Min S-L, Chen T-C, Yashima M. Investigation on strengthening and toughening mechanisms of Ce-TZP/Al₂O₃ nanocomposites. *Metall Mater Trans, A Phys Metall Mater Sci.* 2006;37(6):1969-75. <http://dx.doi.org/10.1007/s11661-006-0139-2>.
25. Nawa M, Nakamoto S, Sekino T, Niihara K. Tough and strong Ce-TZP/alumina nanocomposites doped with titania. *Ceram Int.* 1998;24(7):497-506. [http://dx.doi.org/10.1016/S0272-8842\(97\)00048-5](http://dx.doi.org/10.1016/S0272-8842(97)00048-5).
26. Cutler RA, Mayhew RJ, Prettyman KM, Virkar AV. High-toughness Ce-TZP/Al₂O₃ ceramics with improved hardness and strength. *J Am Ceram Soc.* 1991;74(1):179-86. <http://dx.doi.org/10.1111/j.1151-2916.1991.tb07315.x>.
27. ASTM: American Society for Testing and Materials. ASTM C1327-15: standard test method for Vickers indentation hardness of advanced ceramics. West Conshohocken: ASTM; 2016.
28. Casellas D, Nagl MM, Llanes L, Anglada M. Fracture toughness of alumina and ZTA ceramics: microstructural coarsening effects. *J Mater Process Technol.* 2003;143-144:148-52. [http://dx.doi.org/10.1016/S0924-0136\(03\)00396-0](http://dx.doi.org/10.1016/S0924-0136(03)00396-0).
29. Niihara K. A fracture mechanics analysis of indentation-induced palmqvist crack in ceramics. *J Mater Sci Lett.* 1983;2(5):221-3. <http://dx.doi.org/10.1007/BF00725625>.
30. ASTM: American Society for Testing and Materials. ASTM C1161-13: standard test method for flexural strength of advanced ceramics at ambient temperature. West Conshohocken: ASTM; 2013.
31. Amarante JEV, Pereira MVS, Souza GM, Alves MFRP, Simba BG, Santos C. Roughness and its effects on flexural strength of dental yttria-stabilized zirconia ceramics. *Mater Sci Eng A.* 2019;739:149-57. <http://dx.doi.org/10.1016/j.msea.2018.10.027>.
32. Wu H, Liu W, He R, Wu Z, Jiang Q, Song X, et al. Fabrication of dense zirconia-toughened alumina ceramics through a stereolithography-based additive manufacturing. *Ceram Int.* 2017;43(1, Part B):968-72. <http://dx.doi.org/10.1016/j.ceramint.2016.10.027>.
33. Nawa M, Yamada K, Kurzoe N. Effect of the t-m transformation morphology and stress distribution around the crack path on the measured toughness of zirconia ceramics: a case study on Ce-TZP/alumina nanocomposite. *J Eur Ceram Soc.* 2013;33(3):521-9. <http://dx.doi.org/10.1016/j.jeurceramsoc.2012.10.007>.
34. Kern F, Gadow R. In situ platelet reinforcement of alumina and zirconia matrix nanocomposites - one concept, different reinforcement mechanisms. *Adv Sci Technol.* 2014;87:118-25. <http://dx.doi.org/10.4028/www.scientific.net/AST.87.118>.
35. Gregori G, Burger W, Sergio V. Piezo-spectroscopic analysis of the residual stress in zirconia-toughened alumina ceramics: the influence of the tetragonal-tomonoclinic transformation. *Mater Sci Eng.* 1999;271(1-2):401-6. [http://dx.doi.org/10.1016/S0921-5093\(99\)00383-4](http://dx.doi.org/10.1016/S0921-5093(99)00383-4).
36. Fan K, Ruiz-Hervias J, Pastor JY, Gurauskis J, Baudin C. Residual stress and diffraction line-broadening analysis of Al₂O₃/Y-TZP ceramic composites by neutron diffraction measurement. *Int J Refract Met Hard Mater.* 2017;64:122-34. <http://dx.doi.org/10.1016/j.ijrmhm.2017.01.011>.
37. Casellas D, Ráfols I, Llanes L, Anglada M. Fracture toughness of zirconia-alumina composites. *Int J Refract Met Hard Mater.* 1999;17(1-3):11-20. [http://dx.doi.org/10.1016/S0263-4368\(98\)00064-X](http://dx.doi.org/10.1016/S0263-4368(98)00064-X).